Multiple steady state solutions for a flame stabilized behind a highly conductive bluff body

Vadim N. Kurdyumov, Carmen Jiménez
CIEMAT
Madrid, Spain

1 Introduction

One of the strategies for flame stabilization in a flow of combustible mixture is to place it in the wake of a bluff body, that acts as a flame holder. Systematic studies of this problem can be found in literature since at least 60 years [1–5]. More recently, the use of computational facilities has allowed advances in the understanding of these flame stabilization processes [6–15], but fundamental aspects still remain unexplored.

A series of experimental and numerical studies of a flame stabilized behind a fixed and a rotating cylinder in [7, 9–11] have shown different flame positions, shapes and dynamics when the temperature of the flame holder is forced to change. In a recent study [15], the flame stabilization by means of a solid square maintained at a constant temperature in a laminar channel flow was studied. It was found that for certain values of the parameters, multiple steady-state solutions corresponding to a zero value of the total heat flux on the square surface arise. In this case where multiple solutions are found, it is natural to think that not all of the solutions can be stable.

In the present work we study a flame stabilized by means of an isolated highly conducting circular cylinder placed perpendicularly in a uniform flow. We apply a number of simplifications to the analyses mentioned above, eliminating difficulties related to the square shape of the body or the presence of additional geometric parameters in a channel of finite width, as well as complex chemical kineticss or conjugate heat transfer, so that a parametric analysis is possible. This allows to focus the study on the physical reasons for the appearance of non-unique steady-state solutions and to investigate their stability.

2 Mathematical Formulation and Numerical Treatment

We consider a circular cylinder of radius R perpendicular to an incoming flow of a combustible mixture at initial temperature T_0 and with a uniform velocity U_0 far upstream relative to the cylinder. We assume that the planar flame speed, S_L, is less than the velocity of the mixture, $S_L < U_0$, thus preventing the flame to propagate upstream. Under this condition, flame stabilization is only possible under the action of the cylinder that works like a flame holder.

The sketch of the problem and the coordinate system are shown in Fig.1. For simplicity, the problem is considered two-dimensional and all solutions are assumed to be mirror-symmetric about the x-axis.

Correspondence to: vadim.k@ciemat.es

Thus, all dependent variables are functions of the spatial variables r and φ, where $x = r\cos\varphi$, $y = r\sin\varphi$ and $0 < \varphi < \pi$.

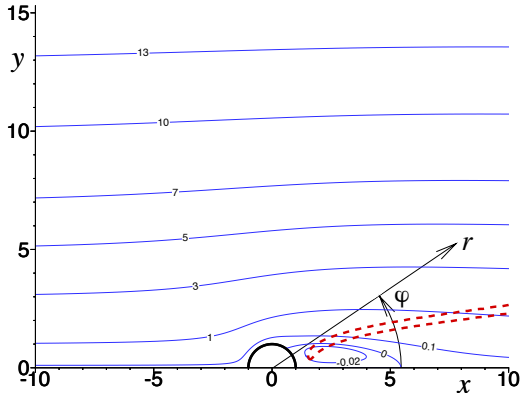

Figure 1: Sketch of the problem, the coordinate system, the illustration of an anchored flame (a dashed-line contour) and stream function isolines (solid lines) calculated for $Re = 20$.

Considering the mixture to be deficient in fuel, the mass of fuel consumed per unit volume and time is given by $\Omega = \mathcal{B}\rho^2 Y \exp(-E/\mathcal{R}T)$, where Y is the fuel mass fraction, $\mathcal{B}$ is a pre-exponential factor, ρ is the density of the mixture, E is the overall activation energy and $\mathcal{R}$ is the universal gas constant.

We consider a diffusive-thermal model, formally assuming that the density of the mixture ρ, the thermal diffusivity $\mathcal{D}_T$, the individual molecular fuel diffusivity D, the heat capacity c_p, and the kinematic viscosity ν are all constant. Consequently, the flow field is not affected by the combustion field and is determined a priori by solving the standard Navier-Stokes equations. The study is limited to thin cylinders and small Reynolds numbers, thus the velocity field is assumed to be independent of time. If the characteristic length and speed are chosen as R and U_0 and the pressure variations are made dimensionless using the dynamic pressure ρU_0^2 , the velocity field $\mathbf{v}$ is determined from

$$\begin{aligned} &(\mathbf{v}\cdot\nabla)\mathbf{v} = -\nabla p + Re^{-1}\Delta\mathbf{v}, \quad \nabla\cdot\mathbf{v} = 0, \\ &r = 1: \quad \mathbf{v} = 0, \qquad r\to\infty: \quad \mathbf{v} = \mathbf{e}_x, \end{aligned} \tag{1}$$

where $Re = RU_0/\nu$ is the Reynolds number.

The combustion field is determined by the coupled energy and fuel balance equations with the velocity field computed from Eqs. (1). In the following, the laminar flame speed of the planar adiabatic flame S_L and the thermal flame thickness defined as $\delta_T = \mathcal{D}_T/S_L$ are used to specify the non-dimensional parameters. The non-dimensional temperature is defined by $\theta = (T - T_0)/(T_e - T_0)$, where $T_e = T_0 + QY_0/c_p$ represents the adiabatic temperature of the corresponding planar flame, and the fuel mass fraction is normalized by its upstream value Y_0. Choosing the convection time R/U_0 as a unit of time, the dimensionless transport equations become

$$\frac{\partial\theta}{\partial t} + (\mathbf{v}\cdot\nabla)\theta = \frac{1}{RePr}\,\Delta\theta + \frac{d}{RePr}\,\omega \tag{2}$$

$$\frac{\partial Y}{\partial t} + (\mathbf{v}\cdot\nabla)Y = \frac{1}{LeRePr}\,\Delta Y - \frac{d}{RePr}\,\omega \tag{3}$$

where $\Delta = \partial^2/\partial r^2 + r^{-1}\partial/\partial r + r^{-2}\partial^2/\partial\varphi^2$ is the Laplace operator and $\omega = \frac{\beta^2}{2Le\,u_p^2} Y \exp\left\{\frac{\beta(\theta-1)}{1+\gamma(\theta-1)}\right\}$ is the dimensionless reaction rate. The factor $u_p = S_L/U_L$ introduced in this expression allows to

accommodate for the difference between the asymptotic value of laminar flame speed obtained for large activation energy ($\beta \gg 1$) and the numerical value S_L for finite β. The numerical values of u_p were reported in [16] as a function of the Lewis number.

The following non-dimensional parameters appear in the above equations: the Zel'dovich number, $\beta = E(T_e - T_0)/\mathcal{R}T_e^2$, the Lewis number, $Le = \mathcal{D}_T/\mathcal{D}$, the heat release parameter, $\gamma = (T_e - T_0)/T_e$, the Prandtl number, $Pr = \nu/\mathcal{D}_T$, the Reynolds number, $Re = U_0 R/\nu$, and the reduced Damkohler number, $d = R^2 S_L^2/\mathcal{D}_T^2$. In this work we assigned the values $\beta = 10$, $\gamma = 0.7$, $Le = 1$ and $Pr = 0.72$.

In this work we assume that the thermal conductivity of the solid material is much higher than that of the gas. In this case the temperature of the cylinder remains uniform and depends only on time. Denoting the temperature of the cylinder as θ_w and the local heat flux on the cylinder surface as $q_L(\varphi) = \partial\theta/\partial r\big|_{r=1}$, the energy balance equation for the cylinder becomes:

$$C\frac{d\theta_w}{dt} = q, \quad \text{where} \quad q = \int_0^\pi q_L \, d\varphi \quad \text{is the total heat flux.} \tag{4}$$

Here C represents the total dimensionless thermal capacity of the cylinder. In realistic cases of metal flame holders, for example, this parameter should be much greater than one.

The boundary conditions for the temperature and mass fraction on the cylinder surface become:

$$0 < \varphi < \pi, \quad r = 1: \quad \theta = \theta_w, \quad \frac{\partial Y}{\partial r} = 0\,. \tag{5}$$

On the x-axis, standard symmetry conditions are assumed:

$$1 < r < \infty, \quad \varphi = 0,\, \pi: \quad \frac{\partial\theta}{\partial\varphi} = \frac{\partial Y}{\partial\varphi} = 0\,. \tag{6}$$

The boundary conditions for the far-field temperature and mass fraction are set as follows:

$$r \to \infty: \quad \begin{cases} \partial^2\theta/\partial r^2 = \partial^2 Y/\partial r^2 = 0\,, & 0 < \varphi < \varphi_*\,. \\ \theta = Y - 1 = 0, & \varphi_* < \varphi < \pi\,, \end{cases} \tag{7}$$

It should be noted that the influence of the far field boundary conditions becomes negligible if the computational domain is chosen large enough. In all calculations presented below we use $\varphi_* = \pi/4$. This value was varied without any substantial differences in the results.

The steady Navier-Stokes Eqs. (1), written in terms of the stream function ψ defined from the relations $v_r = r^{-1}\partial\psi/\partial\varphi$, $v_\varphi = \partial\psi/\partial r$ and the vorticity $\zeta = \partial v_r/\partial\varphi - \partial(r\,v_\varphi)/\partial r$, were solved numerically using a Gauss-Seidel method with over-relaxation.

Steady as well as time-dependent computations of Eqs. (2)-(3) were carried out in a finite domain, $1 < r < r_{max}$, with the typical value $r_{max} = 10 \div 15$. Changing the domain size within these limits did not lead to noticeable changes in the results for the temperature and mass fraction fields. The calculations of the velocity field are more sensitive to the size of the domain and therefore were carried out for $r_{max} = 30 \div 50$. The typical number of grid points was 1001×301 (this was doubled in some cases without significant differences in results).

In order to determine steady (but not necessary stable) solutions, the steady counterparts ($\partial/\partial t \equiv 0$) of Eqs. (2)-(3) were solved using a Gauss-Seidel method with over-relaxation. For unsteady calculations an explicit marching procedure was used with first order discretization in time. The typical time step was $\tau = 10^{-4} \div 10^{-5}$. No significant differences were found in the results when τ was halved.

3 Steady State Solutions

One can see from Eq. (4) that the steady-state solutions ($\partial/\partial t \equiv 0$) satisfy the condition $q = 0$. In these cases, the cylinder temperature, θ_w, should be found as part of the solution and the value of C does not affect it. The following procedure was used: First, the steady-state counterpart of Eqs. (2)-(3) was calculated for a fixed cylinder temperature. After that, the value of q given by Eq. (4) was considered as a function of θ_w.

The results for $Re = 20$ and different values of d are shown in Fig. 2 left. For small Damköhler numbers the cylinder temperature corresponding to the steady-state condition $q = 0$ is unique and found around $\theta_w \approx 0.15$, as the curve with $d = 5$ shows. For larger values of d, as for $d = 10$, two additional steady-state solutions appear, one with an intermediate temperature and another one with a cylinder temperature close to adiabatic. For $Re = 20$, the emergence of these two states occurs at $d \gtrsim 7.05$. With a further increase in d, two additional roots of the equation $q = 0$ appear. This is illustrated by the curve with $d = 20$ and occurs approximately in for $19.6 \lesssim d \lesssim 23.2$. Thus, in this interval of d, there are five steady-state solutions. These solutions are indicated by open circles and the letters "a, b, c, d, e" in Fig. 2 left. These additional roots then disappear for $d \gtrsim 23.2$. Finally, with a further increase in d, the steady-state with a relatively cold cylinder disappears and the only steady state presents a cylinder temperature close to adiabatic. This happens at $d \gtrsim 56.3$. It is obvious that all the critical values of the Damköhler number given here depend on other parameters, in particular, on the Reynolds number.

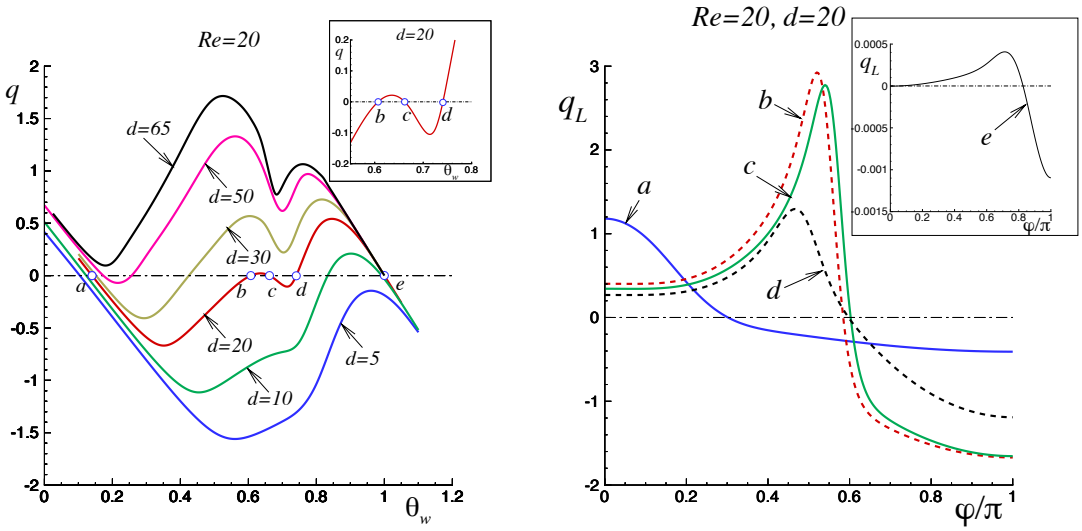

Figure 2: Left: The calculated q values given by Eq. 4 plotted as a function of θ_w for $Re = 20$ and various d. Right: Local heat flux distribution on the cylinder surface calculated for the solutions "a","b","c","d" and "e" marked with open circles.

The flame structure for different values of the Damkohler number is illustrated in Fig. 3 for $d = 20$. The solution corresponding to point "a" in the left figure is characterized by a relatively cold cylinder temperature and a flame located behind the cylinder. For solution "e", for which the temperature of the cylinder is very close to the adiabatic temperature, the flame originates in front of the cylinder and surrounds it. For other solutions, intermediate configurations are found.

The local heat flux $q_L = \partial\theta/\partial r|_{r=1}$ along the surface of the cylinder is shown in Fig. 2 right as a function of φ (note that $\varphi = 0$ corresponds to the rear point of the cylinder). For all solutions "a"-"e" the cylinder is heated ($q_L > 0$) through its rear and cooled ($q_L < 0$) through the front. It is noticeable that the heat flux q_L is very small for the "e" solution compared to the other cases.

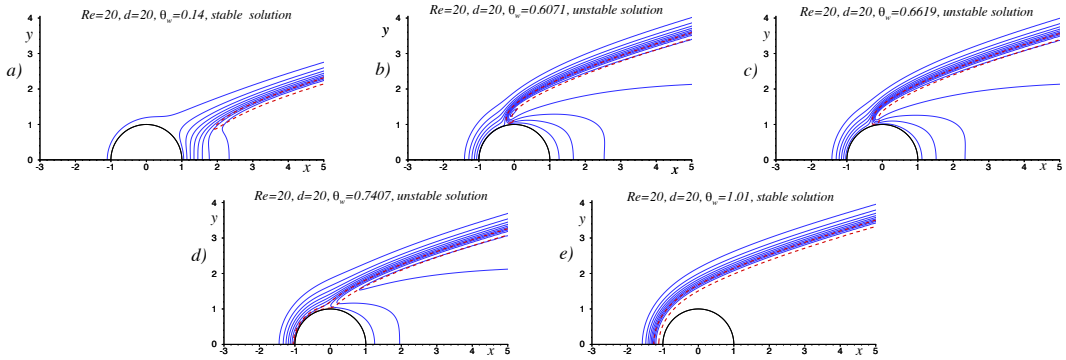

Figure 3: Temperature distributions (solid lines, in an interval 0.1) and the reaction rate isoline (a dashed line, plotted for $\omega = 10$) for the steady-state solutions marked with open circles "a", "b", "c", "d" and "e" in Fig. 2, for $Re = 20$ and $d = 20$.

4 Stability and Time-Dependent Dynamics

In order to check the above steady-state solutions for stability, time-dependent Eqs. (2)-(3) and (4) were calculated for different values of the parameter C. The temperature and mass fraction distributions obtained for solutions b, c, and d were chosen as initial conditions. The time histories of θ_w are plotted in Fig. 4, showing that after an oscillatory transition, the solution approaches one of the states "a" or "e". Thus, numerical simulations show that states "b", "c", and "d" are unstable, while states "a" and "e" are stable. This is indicated in Fig. 3.

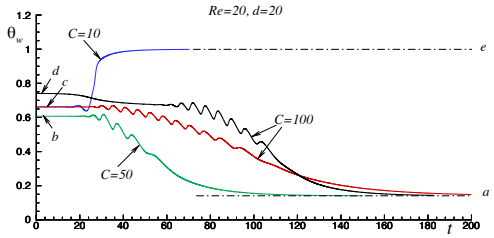

Figure 4: Time histories of the cylinder temperature calculated for $Re = 20$, $d = 20$ and several values of C. Steady-state distributions "b", "c", and "d" were chosen as the initial distributions for temperature and mass fraction. Dash-dotted lines indicate temperatures for stable states "a" and "e".

5 Summary and Discussion

This study of flame stabilization by a cylindrical isolated bluff body, showed that there is an interval of combustion reaction intensity (controlled by the Damköhler number) within which the problem has multiple steady-state solutions. The total number of different non-trivial steady-states, that is, solutions involving combustion, can reach five plus a trivial cold state without flame. Outside of this interval of Damköhler numbers, within which there is a multiplicity of solutions, only one nontrivial steady-state solution remains.

Numerical analysis shows that at least two stationary states are stable. For the first stable solution, the flame spreads out behind the cylinder and its temperature is relatively low. For the other stable solution, the cylinder is heated to a high temperature close to the adiabatic temperature of the mixture and the flame is located around the cylinder.

References

[1] F.H. Wright, Some aerodynamics factors influencing bluff body flame stabilization, *Combust. Flame* 2 (1958) 96-97.

[2] F.H. Wright, Bluff-body flame stabilization - blockage effects, *Combust. Flame* 3 (1959) 319-337.

[3] T. Maxworthy, On the mechanism of bluff body flame stabilization at low velocities, *Combust. Flame* 6 (1962) 233-244.

[4] K.M. Kundu, D. Banerjee, D. Bhaduri, Theoretical analysis on flame stabilization by a bluff-body, *Combust. Sci. Tech.* 17 (1977) 153-162.

[5] K.M. Kundu, D. Banerjee, D. Bhaduri, On flame stabilization by bluff-bodies, *J. Eng. Power* 102 (1980) 209-214.

[6] A. Fan, J. Wan, K. Maruta, H. Yao, W. Liu, Interactions between heat transfer, flow field and flame stabilization in a micro-combustor with a bluff body, *Int. J. Heat Mass Trans.* 66 (2013) 72-79.

[7] M. Miguel-Brebion, D. Mejia, P. Xavier, F. Duchaine, B. Bedat, L. Selle, T. Poinsot, Joint experimental and numerical study of the influence of flame holder temperature on the stabilization of a laminar methane flame on a cylinder, *Combust. Flame* 172 (2016) 153-161.

[8] K. Kedia, A. Ghoniem, The anchoring mechanism of a bluff-body stabilized laminar premixed flame, *Combust. Flame* 161 (2014) 327-339.

[9] P. Xavier, A. Ghani, D. Mejia, M. Miguel-Brebion, M. Bauerheim, L. Selle, T. Poinsot, Experimental and numerical investigation of flames stabilised behind rotating cylinders: interaction of fames with a moving wall, *J. Fluid Mech.* 813 (2017) 127-151.

[10] D. Mejia, M. Bauerheim, P. Xavier, B. Ferret, L. Selle, T. Poinsot, Stabilization of a premixed laminar flame on a rotating cylinder, *Proc. Combust. Inst.* 36 (2017) 1447-1455.

[11] D. Mejia, M. Miguel-Brebion, A. Ghani, T. Kaiser, F. Duchaine, L. Selle, T. Poinsot, Influence of flame-holder temperature on the acoustic flame transfer functions of a laminar flame, *Combust. Flame* 188 (2018) 5-12.

[12] C. Jiménez, D. Michaels, A. Ghoniem, Stabilization of ultra-lean hydrogen enriched inverted flames behind a bluff-body and the phenomenon of anomalous blow-off, *Combust. Flame* 191 (2018) 86-98.

[13] C. Jiménez, D. Michaels, A. Ghoniem, Ultra-lean hydrogen-enriched oscillating flames behind a heat conducting bluff-body: Anomalous and normal blow-off, *Proc. Combust. Ins.* 37 (2019) 1843-1850.

[14] V.N. Kurdyumov, Y.L. Shoshin, L.P.H. de Goey, Structure and stability of premixed flames stabilized behind the trailing edge of a cylindrical rod at low Lewis numbers, *Proc. Combust. Ins.* 35 (2015) 981-988.

[15] S. Berger, F. Duchaine, L.Y.M. Gicquel, Bluff-body thermal property and initial state effects on a laminar premixed flame anchoring pattern, *Flow Turb. Combust.* 100 (2018) 561-591.

[16] V.N. Kurdyumov, Lewis number effect on the propagation of premixed flames in narrow adiabatic channels: Symmetric and non-symmetric flames and their linear stability analysis, *Combust. Flame* 158 (2011) 1307-1317.